Temporal Variability of Fair-Weather Cumulus Statistics at the ACRF SGP Site

LARRY K. BERG AND EVGUENI I. KASSIANOV

Pacific Northwest National Laboratory, Richland, Washington

(Manuscript received 2 October 2007, in final form 10 December 2007)

ABSTRACT

Continental fair-weather cumuli exhibit significant diurnal, day-to-day, and year-to-year variability. This study describes the climatology of cloud macroscale properties, over the U.S. Department of Energy's Atmospheric Radiation Measurement (ARM) Climate Research Facility (ACRF) Southern Great Plains (SGP) site. The diurnal cycle of cloud fraction, cloud-base height, cloud-top height, and cloud thickness were well defined. The cloud fraction reached its maximum value near 1400 central standard time. The average cloud-base height increased throughout the day, while the average cloud thickness decreased with time. In contrast to the other cloud properties, the average cloud-chord length remained nearly constant throughout the day. The sensitivity of the cloud properties to the year-to-year variability of precipitation and day-to-day changes in the height of the lifting condensation level (z_{LCL}) and surface fluxes were compared. The cloud-base height was found to be sensitive to both the year, z_{LCL}, and the surface fluxes of heat and moisture; the cloud thickness was found to be more sensitive to the year than to z_{LCL}; the cloud fraction was sensitive to both the low-level moisture and the surface sensible heat flux; and cloud-chord length was sensitive to z_{LCL}. Distributions of the cloud-chord length over the ACRF SGP site were computed and were well fit by an exponential distribution. The contribution to the total cloud fraction by clouds of each cloud-chord length was computed, and it was found that the clouds with a chord length of about 1 km contributed most to the observed cloud fraction. This result is similar to observations made with other remote sensing instruments or in modeling studies, but it is different from aircraft observations of the contribution to the total cloud fraction by clouds of different sizes.

1. Introduction

While fair-weather clouds (FWC) are small in size, they play an important role in the earth's climate (e.g., Stull 1992). FWC increase the planetary albedo and decrease the shortwave radiation at the surface, while having little influence on the infrared radiation budget. These clouds are ubiquitous, occurring over large areas of continents and trade wind regions over oceans (Warren et al. 1988). For example, Stull (1992) found that cumuli contributed about 33% of the summertime cloud cover over Madison, Wisconsin.

FWC form when the boundary layer depth grows larger than the height of the lifting condensation level (z_{LCL}) (e.g., Wilde et al. 1985). The boundary layer depth is controlled by the interplay of the surface sensible heat flux, the static stability of the atmosphere above the boundary layer, and large-scale subsidence or lifting, while z_{LCL} quantifies the amount of moisture in the boundary layer. For example, Ray et al. (2003) reported that formation of FWC was closely linked to the surface moisture flux and the soil moisture. In contrast, Rabin et al. (1990) described that clouds formed first in regions with large sensible heat fluxes. Chagnon et al. (2004) reported that FWC are enhanced over both deforested patches and elevated terrain in the Amazon basin. Betts (2004) and Betts and Viterbo (2005) have found that the surface sensible and latent heat fluxes and the soil moisture computed in the European Centre for Medium-Range Weather Forecasts (ECMWF) reanalysis are related to the cloud-base height (CBH) and cloud fraction (CF). Peppler and Lamb (1989) focused on precipitating clouds, and determined that z_{LCL} was the best predictor of convective precipitation over the central United States.

Because of their small size, on the order of a kilometer, FWC are subgrid-scale in most numerical models of the atmosphere. Many detailed studies, such as those conducted by the Global Energy and Water Cycle Experiment (GEWEX) Cloud System Study and even new

Corresponding author address: Dr. Larry K. Berg, Pacific Northwest National Laboratory, K9-30, Richland, WA 99352.
E-mail: larry.berg@pnl.gov

DOI: 10.1175/2007JCLI2266.1

approaches, like the MultiScale Modeling Framework, in which two- or three-dimensional cloud resolving models are run inside each GCM grid box (Randall et al. 2003), do not explicitly resolve FWC. Therefore a parameterization for these clouds is still required.

A comprehensive FWC climatology is needed for the verification of new FWC parameterization schemes. For example, Berg and Stull (2005) developed a new parameterization for FWC that predicts the cloud properties, such as the CBH, cloud-top height (CTH), and CF. Preliminary testing of the new scheme used data collected during a field campaign conducted during the summer of 1996 (Stull et al. 1997). This campaign included a relatively small number of research flights conducted over three locations within the Atmospheric Radiation Measurement (ARM) Climate Research Facility (ACRF) Southern Great Plains (SGP) site. To more rigorously evaluate this and other schemes, new datasets are needed to quantify the seasonal statistics of FWC at various sites around the globe.

A number of cloud climatologies have been completed for the ACRF SGP site, but these efforts have focused on either broad categories of clouds grouped by height and season (e.g., Lazarus et al. 2000) or height and time of day (e.g., Dong et al. 2005). In these two examples, the low clouds were not separated by the type of cloud, either stratiform or cumuliform, nor were the horizontal cloud-chord lengths (CCL: the length of the cloud slice that passed directly overhead) of the clouds reported. Lane et al. (2002) presented distributions of CCL, but only for one year. Other studies (e.g., Plank 1969; Cahalan and Joseph 1989; Rodts et al. 2003) have computed distributions of CCL for specific case-study periods. In their work, Rodts et al. (2003) computed the contribution to the CF of clouds with various CCL and found that, albeit for only four days over Florida, the smallest clouds contributed the most to the CF. In contrast, other studies that made use of either aircraft photos or satellite images (e.g., Plank 1969; Wielicki and Welch 1986; Sengupta et al. 1990) demonstrated that moderately sized clouds made the most significant contribution to the CF. These differences could be related to the small number of days sampled by Rodts et al. (2003) or to the different sampling techniques employed in these studies. The work presented here addresses these shortcomings by looking explicitly at the temporal variation of FWC over five summers from 2000 to 2004, inclusive, derived using data from a suite of ground-based instruments. Specifically, the following questions will be addressed:

1) What are the diurnal variations in the cloud macrophysical properties such as CF, CBH, CTH, cloud thickness (CTK), and CCL?
2) How does the year-to-year variability in precipitation and day-to-day variability in surface fluxes and z_{LCL} affect the cloud macrophysical properties?
3) How do clouds with different CCLs contribute to the CF?

In the following section, the methodology used to determine the cloud properties will be defined. The classification of the meteorological conditions will be described in section 3. The results will be presented in section 4, followed by a discussion of our findings in section 5.

2. Methodology

This study includes data obtained during the summers (defined to include May–August) of 2000 through 2004. Data were collected at the ARM ACRF SGP Central Facility (hereafter called the Central Facility) located in north-central Oklahoma (Stokes and Schwartz 1994). The instruments at Central Facility that were used in this study include 35-GHz cloud radar, laser ceilometer, microwave radiometer, and micropulse lidar, along with a complete suite of instruments to measure the downwelling radiation, surface fluxes of heat and moisture, and standard meteorological variables, including a 915-MHz radar wind profiler. The measurements from the cloud radar, laser ceilometer, microwave radiometers, and micropulse lidar were combined in the ARM Active Remotely Sensed Clouds Locations (ARSCL) value-added product (VAP) to provide the best estimate of cloud boundaries, including the CBH and CTH (Clothiaux et al. 2000). The time resolution of this product is 10 s, and the vertical resolution is a function of the sensor used to determine the cloud boundary. The vertical resolution of the laser ceilometer is 7.6 m, while the resolution of the micropulse lidar is 30 m. The 90-m vertical resolution of the cloud radar is coarser than either of the optical instruments. Output from this VAP includes a flag indicating if the cloud radar or micropulse lidar was used to determine the cloud top. Values of CTH determined from the lidar are very uncertain because of attenuation of the laser by the cloud; therefore, only cases in which the CTH was determined from the cloud radar were included in the analysis of CTH and CTK. These measurements all have a narrow field of view, so some errors in the measured cloud parameters are expected over short time intervals (e.g., Kassianov et al. 2005; Berg and Stull 2002). For example, work by Berg and

Stull (2002) suggested that for 1-h averages of cloud cover collected by a point sample, one might expect the random error in cloud amount to be on the order of 10%. But, by averaging over many days, the random error is significantly reduced.

The first task in the development of the climatology of FWC was to identify days on which there were FWC, and the second task was the determination of the cloud macrophysical properties. An attempt was made to use the cloud amount computed from the ARSCL VAP time series to determine the cloud type. This methodology is similar to that applied by Wang and Sassen (2001), but focused on only fair-weather cumuli. However, there is a significant amount of noise in the hour averages of cloud cover, which make application of such a method difficult. Other methods were considered to identify cases with FWC. Duchon and O'Malley (1999) suggested that the irradiance could be used to identify the cloud type. To use their method, the measured irradiance must be scaled by the clear-sky value and the standard deviation of the irradiance computed. Duchon and O'Malley (1999) suggested that cases in which the standard deviation is greater than 100 W m^{-2} indicates that there are cumuli. However, this method erroneously suggested that there were cumuli on virtually every day of the summer at the Central Facility.

The first task was divided into two steps: the ARSCL VAP was used to identify days that might have FWC with a simple rule-based approach, and then movies from the Total Sky Imager (TSI) were used to check each day identified in the first step. The TSI consists of a vertically pointing hemispheric camera that records a high-resolution image of the sky every 30 s. Data from this instrument can be used to infer a number of features about the cloud field, but was simply applied here to confirm that presence of FWC on the days of interest.

In the first step, 1-h averages of CBH, CTH, and CTK were computed from the original time series. The averaged ARSCL VAP time series was searched for days with the expected characteristics of FWC (Berg and Stull 2002). In particular, the CBH was required to be between 0.3 and 3 km. Cases in which the clouds appeared to be forced by the large-scale circulation—in other words, cases with large amounts of high clouds—were excluded to focus on cases in which the clouds are forced by solar heating of the surface. Use of the CBH criteria resulted in observations from four days out of the 5-yr period to be excluded from the analysis because of cloud base criteria. Because of the small number of cases involved application of these criteria should have minimal effect on the results presented here. In the second step, TSI images were used to eliminate days identified in the first step in which there was agricultural burning, high clouds, or cases in which the FWC changed to stratocumulus. The methodology used is labor intensive because of the number of TSI images that were inspected, but provides a robust multiyear dataset. The third step of our analysis involved calculating the cloud statistics from the ARSCL VAP data stream for selected days.

a. Average CBH, CTH, and CTK

Once the days with FWC were identified, the time series from the ARSCL VAP was used to compute the average CBH and CTH over each hour interval in order to evaluate the diurnal evolution of these variables. Daily averages of CBH and CTH were also computed to evaluate the year-to-year and day-to-day variability. CTK was computed by taking the difference between the CTH and the CBH for each observation with a good estimate of CTH. These statistics could be influenced in cases in which the clouds were tilted with height or in instances in which only the edge of the cloud passes over the radar and/or lidar beams.

b. Average CF

The CF has traditionally been defined in two different ways. One method is based on the amount of the sky dome that is covered with clouds, and is also called the sky cover. This is the hemispherical measure of CF made by a human observer on the ground. This measure includes some contribution to the CF by the sides of cumuli (Kassianov et al. 2005). The other method is based on the projection of clouds onto the surface of the earth. This is the CF (also called the earth cover) measured by a satellite or zenith-looking instrument (or suite of instruments in the case of the ARSCL VAP time series), or by an aircraft passing horizontally through a field of FWC. In this study, we will use the latter measure as the CF. This value of CF can be measured in two ways: based on the fraction of time that a cloud is overhead, which will be called the *temporal* CF, or based on the ratio of the sum of the CCLs during a time interval to the total distance of a cloud field that moves over the sensor in that time interval, which will be called the *spatial* CF. The former only requires data from the ARSCL VAP, while the latter requires knowledge of the wind speed at the cloud altitude to determine the CCL. The spatial CF has been defined formally by Rodts et al. (2003), in terms of the cloud fraction density, α_f, which they defined as

$$\alpha_f(l) = \frac{1}{L} n(l) \times l, \tag{1}$$

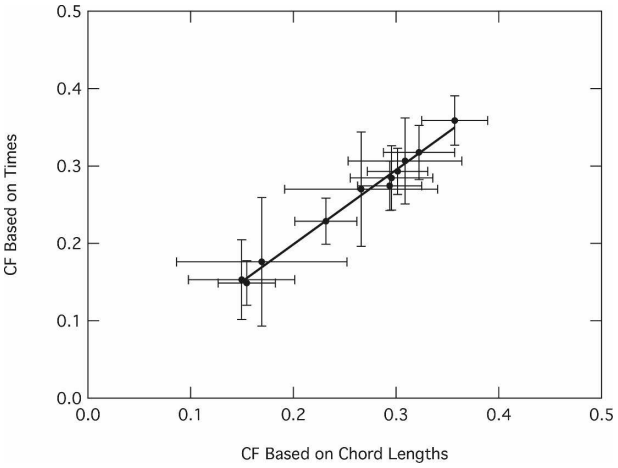

FIG. 1. Cloud fraction determined from the clear and cloudy chord lengths vs the CF determined from the time intervals with clouds over the Central Facility. The thick line is the least squares best fit.

where n is the number of clouds with a given CCL, l is the CCL, and L is the total length of interest. The advantage of α_f is that it quantifies the CF associated with a given CCL and is discussed in more detail in section 5c. The total CF can then be defined as

$$\mathrm{CF} = \int_{l_{\min}}^{l_{\max}} \alpha_f(l)\, dl, \tag{2}$$

where $l_{\min}$ and $l_{\max}$ are the minimum and maximum CCL used to determine the CF. Owing to errors associated with the determination of CCL (which are described in the next section), $l_{\min}$ and $l_{\max}$ were set to 0.1 and 6 km, respectively. In this study both temporal and spatial methods have been used to quantify the CF. If the wind speed was constant, then these methods give the same result, and both methods fail when the wind speed becomes sufficiently small so that clouds are no longer transported over the sensor. In addition, each method assumes that the CF does not change during the averaging period. The method of choice is a function of either application or the measurement method. For example, if one is concerned about the amount of solar radiation that is available at a certain point at the surface, then the CF based on the amount of time that a cloud is overhead (or more precisely blocking the direct solar beam) is of interest. Overall, there is good agreement in the CF measured using both methods (Fig. 1). Indeed, the slope of the least squares best-fit line is 0.96. In each case the measurement error was determined using Eq. (10) from Berg and Stull (2002) and was a function of the cloud cover and the time or total chord length. The agreement between the two methods was also compared for the three z_{LCL} groups (not shown), and the differences in the two values of CF were consistent with the results shown in Fig. 1.

c. Average CCL

In this study, the CCL is defined as the length of a slice of cloud that passes through the cloud radar or lidar beams. This value is the product of the length of time that a cloud is intercepted by the radar or lidar beam and the wind speed at which the cloud is moving through the beam. The length of time over the sensors was simply computed by the number of sequential ARSCL VAP observations that showed a cloud overhead. No adjustment was applied to account for short breaks that might occur due to an irregular cloud boundary. The wind speed at cloud-base height was determined from the 915-MHz radar wind profiler operated close to the cloud radar at the Central Facility.

Some additional processing was applied to the data series used to determine the CCL. There was a significant amount of uncertainty in the measurements of CCL for small values of CCLs. The time resolution of the ARSCL VAP is 10 s, and the nominal error of the wind speed measured with the wind profiler is ± 1 m s^{-1}. These two uncertainties can be combined to give the fractional error, which could be as large as 250% when either the CCL or the wind speed is small. Therefore, CCL values of less than 100 m are ignored in the analysis of the CCL. One additional criterion was applied, namely that the CCL must be less than 6 km. Long CCLs could be due to a number of factors: clouds that are separated by less than 10 s in time, clouds that are tilted and hence overlap when viewed from the surface, or clouds that are starting to merge together. Excluding observations that fit these criteria reduces the number of data points by about 13%. One additional adjustment was made for the small number of cases in which the CBH was above the highest altitude wind reported by the radar at its low power setting. Use of data from the low power setting was selected to optimize the vertical resolution of the radar data. In this case, the radar time series was checked and, if there was a good wind speed value near an altitude of 0.5 km, then that value was used as the cloud-base wind speed.

3. Classification of meteorological conditions

Previous investigations have suggested that soil moisture and surface fluxes of sensible and latent heat play an important role in determining the properties of the FWC (e.g., Rabin et al. 1990; Ray et al. 2003; Chagnon et al. 2004). Other authors (e.g., Peppler and Lamb

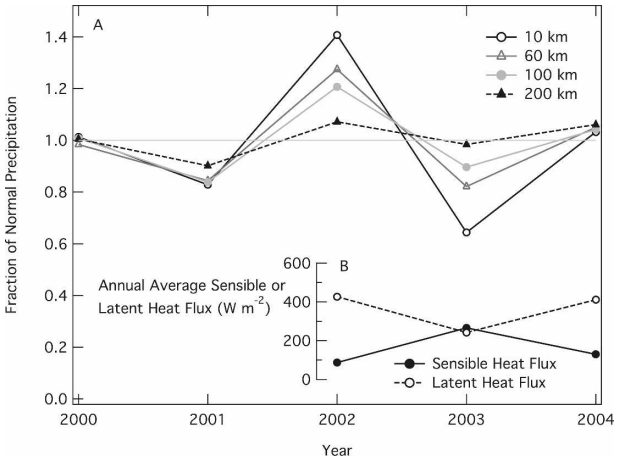

FIG. 2. (a) Fraction of normal (10-yr average) summertime precipitation measured within 10, 60, 100, and 200 km of the Central Facility during the summers of 2000 through 2004 and (b) annual average sensible and latent heat fluxes for the summers of 2002, 2003, and 2004.

1989) have suggested that z_{LCL} is related to the cloud properties. Therefore, we will use three classification methods to group the cloud properties, including

- yearly precipitation,
- the surface fluxes of sensible and latent heat, and
- the z_{LCL} measured by the surface meteorological station at the Central Facility.

Grouping the cloud data by years allows us to evaluate the effect of the year-to-year variability of the precipitation on the FWC, while grouping by z_{LCL} and surface fluxes allows us to evaluate the relative importance of the day-to-day variations.

Wet and dry years at the ACRF SGP have been determined according to the amount of precipitation that has fallen in the vicinity of the Central Facility. The amount of precipitation at the Central Facility, particularly summertime precipitation, is highly variable in space and time. Rather than using the rain gauge at the Central Facility or attempting to interpolate the precipitation using a network of rain gauges, we have used a gridded precipitation dataset generated by the Arkansas–Red River Basin Forecast Center (ABRFC). This dataset combines data from rain gauges with the precipitation estimated by the Weather Surveillance Radar-1988 Doppler (WSR-88D) radars using the process 1 algorithm (Young et al. 2000; Wang et al. 2000) interpolated to a 4×4 km^2 grid. A number of different averages are presented in Fig. 2, which highlights the spatial inhomogeneity of the precipitation. The different averages displayed in Fig. 2 are averages computed for circles of 10, 60, 100, and 200 km diameter centered on the Central Facility. As the circles get larger the interannual variability of the average precipitation decreases. Both the summers of 2001 and 2003 were relatively dry, with less than normal precipitation falling within 50 km of the Central Facility. In this study the normal precipitation is defined as the 10-yr (1995–2004) average of precipitation over the entire ABRFC domain. The precipitation measured during 2001 was 80% of normal, while during 2003 the precipitation measured within 10 km of the Central Facility was 64% of normal. In both cases there was a significant amount of precipitation in May, while the June–August precipitation was less than 50% of normal. These summers will be referred to as the dry summers. In contrast, the precipitation during the summer of 2002 was 110% of normal, and the precipitation during the summer of 2004 was close to normal.

The surface fluxes of sensible and latent heat were obtained from the Energy Balance Bowen Ratio (EBBR) station at the ARCF SGP Central Facility. EBBR stations estimate the 30-min averages of fluxes using the net radiation, the gradients of temperature and moisture, and the soil heat flux. Unfortunately, the data from the summers of 2000 and 2001, along with parts of the summer of 2004, were unavailable due to issues with the instrument at the Central Facility. The surface fluxes have a significant diurnal variation; therefore, rather than the 30-min averages or the daily average value, the average values from 1300–1400 CST were used. These values are generally close to the daily maximum values of both the sensible and latent heat flux. Tests were conducted using data from other periods and the results were not significantly changed. Of the summers for which there was reliable surface flux data, 2002 had the most precipitation and the smallest averaged sensible heat flux (87 W m^{-2}) and the largest latent heat flux (427 W m^{-2}), while 2003 had the least precipitation and the largest annual averaged sensible heat flux (266 W m^{-2}) and the smallest annual averaged latent heat flux (242 W m^{-2}; Fig. 2).

In addition to the relative wetness or dryness of a season and the surface fluxes, z_{LCL} can influence the cloud macroscale properties. Other authors (e.g., Wilde et al. 1985; Peppler and Lamb 1989) have related the observed clouds or precipitation to the thermodynamic structure of the environment. Indeed, Peppler and Lamb (1989) found that z_{LCL} was as useful as a predictor of summertime precipitation as any of the conventional stability indices. In this study values of z_{LCL} were computed from the Surface Meteorological Station (SMOS) located at the Central Facility. The SMOS measures the temperature and humidity 2 m above the surface. The value of z_{LCL} was computed using the ex-

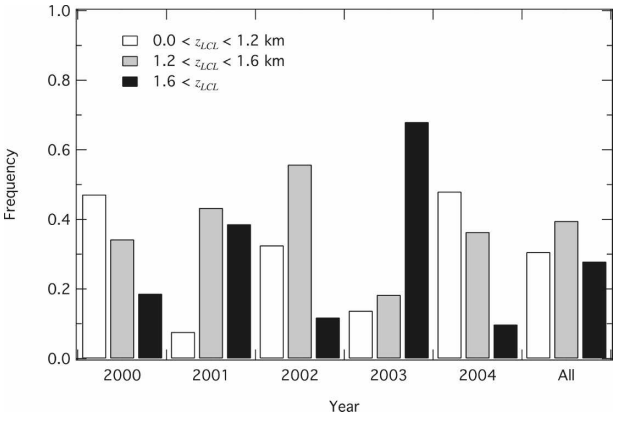

FIG. 3. Relative frequency of hours with small, moderate, or large values of z_{LCL} for the summers 2000 through 2004. The All category is the frequency for all five summers.

pression $z_{\mathrm{LCL}} = 125(T - T_D)$, which is determined from the average lapse rates of both temperature (T) and dewpoint temperature (T_D) (e.g., Bohren and Albrecht 1998).

In this study, the cloud observations were divided into three groups based on the measured value of z_{LCL}: values of z_{LCL} less than 1.2 km, values of z_{LCL} between 1.2 and 1.6 km, and values of z_{LCL} greater than 1.6 km. These values were selected based on the mean and standard deviation of z_{LCL} observed on all of the days that were identified to have FWC at the Central Facility. The mean z_{LCL} for the 5-yr study period was 1.4 km and the standard deviation was 0.7 km. The distribution of z_{LCL} was nearly Gaussian (not shown), so setting the critical values of z_{LCL} to the mean plus or minus the standard deviation left very few cases with large or small z_{LCL}. Therefore, approximately plus or minus one-third of the standard deviation was used to define the critical values of z_{LCL}. Defining the z_{LCL} groups is complicated to some extent by the diurnal evolution of z_{LCL}, which was one reason to use the daily average statistics when evaluating the year-to-year and day-to-day variability. Sensitivity tests were conducted with other ranges of z_{LCL}, and the results were not changed significantly.

While each year had cases within each z_{LCL} category, the number of cases were not evenly distributed (Fig. 3). Not surprisingly, the two driest years had the most cases in which z_{LCL} was greater than 1.6 km. But in these years there were still a significant number of cases in which the value of z_{LCL} was less than 1.2 km. Indeed, almost 15% of the observed cases in 2003 had a value of z_{LCL} less than 1.2 km. The wettest year at the Central Facility was the summer of 2002. While there were a large number of cases with z_{LCL} less than 1.2 km during the summer of 2002, about 12% of the cloudy

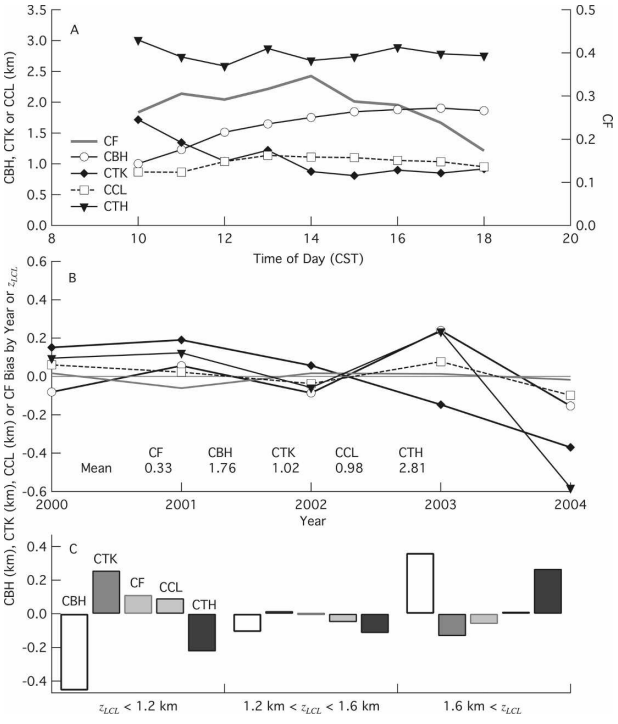

FIG. 4. (a) The 5-yr mean ARSCL VAP values of CF (gray line), CBH (line with circles), CTK (line with diamonds), and CCL (squares with broken line); (b) their average daily bias for each year; and (c) each z_{LCL} group.

cases had a value of z_{LCL} greater than 1.6 km. Thus, we see that in any given year there are cases in which the z_{LCL} is small, moderate, or large.

4. Results

a. Diurnal evolution

The average CBH as a function of time was computed for each day with FWC (section 2). On average, the CBH increases throughout the day until 1700 CST (Fig. 4a). This change is associated with the general increase in value of z_{LCL} during the day. The rate of increase in CBH is larger in the late morning and decreases in the afternoon. Clouds generally start to form between 0900 and 1000 CST, with a peak in CF near 1400 CST. After 1400 the CF decreases until the FWC disappear near 1800 CST. The change in average CF is not symmetrical about the peak in the average CF, the increase between 1000 and 1400 CST is gradual compared to the decrease after 1400 CST.

While the average CBH changes significantly throughout the day, the average CTH does not (Fig. 4a). The nearly constant average value of CTH and the increasing CBH indicate that the average CTK (which is computed by subtracting the CBH from the CTH)

tends to decrease during the day (Fig. 4a). There are a number of important factors that control the CTH, including the mean subsidence rate and the static stability within and above the cloud layer. Berg and Stull (2005) showed that the CTH is well predicted by the convective available potential energy (CAPE) and the stability of the cloud layer when the thermodynamic properties of the boundary layer air parcels are properly accounted for. However, in this study there was only a weak relationship between CTH, CAPE, and the convective inhibition energy (CINE) measured from the radiosondes launched at the Central Facility (not shown). One reason for the difference between this study and the study by Berg and Stull (2005) are the methods used to measure the profiles of temperature and moisture. Radiosonde measurements of boundary layer depth are subject to significant error (e.g., Stull 1988), which leads to large errors in the predicted CAPE and CINE values. In contrast, profiles measured with aircraft sample through many thermals and are subject to less sampling error. Other sources of uncertainty include the role of large-scale dynamics on the cloud fields and the coarse time resolution of the radiosondes (launched at 1130 and 1730 CST).

The average CCL is nearly constant throughout the day, remaining very close to 1 km. (Fig. 4a). This result has some important implications for the interpretation of the average CF as a function of time. The CF can increase in three different ways: because the clouds grow in horizontal size (the number of clouds is fixed), because there are more clouds (the CCL is fixed), or some combination of the two. The nearly constant value of CCL suggests the diurnal increase in CF occurs because the number of clouds increases. Likewise, it shows that the cloud size is not related to the CBH or the boundary layer depth, both of which grow as a function of time. A more detailed analysis of the relationships between the CCL and the CF is presented in section 5c.

b. Year-to-year variability of precipitation

We expect that the daily average CBH would be larger during dry years compared to wet years (e.g., Stull and Eloranta 1985). Indeed, the summers of 2001 and 2003 were relatively dry at the Central Facility and had some of the highest daily average CBHs, while the years with more rainfall had the smallest CBHs (Fig. 4b), as indicated by the positive and negative bias. In this study the bias is defined as the difference between the average daily value for each year and the 5-yr daily mean. While the CTK does show significant year-to-year variability, there does not seem to be a strong relationship between CTK and the amount of precipitation near the ACRF Central Facility. This is indicative of the dependence of the CTK on the stability above the boundary layer, which is influenced by the synoptic conditions. In particular, the clouds observed during the summer of 2004 were significantly shallower, on average, than the clouds measured during any other year. During the summer of 2004, there were a relatively small number of thick clouds. The range of static stability above the boundary layer during the summer of 2004 was similar to that measured in the other summers, so it is unlikely the small number of thick clouds is related to the stability alone. This result highlights the importance of using multiple years when studying FWC. The cloud fraction as a function of year shows some changes, but these changes are relatively small (absolute bias less than 15% cloud cover fraction). Like the CF, the CCL does not change much from year to year and is insensitive to the relative wetness or dryness of the year (Fig. 4b).

c. Cloud sensitivity to z_{LCL}

As shown in Fig. 4c, there are large variations in the daily average CBH associated with changes in the z_{LCL}. There is good agreement between the value of z_{LCL} computed from the dewpoint depression measured by the SMOS and the minimum cloud-base height measured during each averaging period determined from the ARSCL VAP (Fig. 5). These results support the findings of others that z_{LCL} computed from near-surface values is a good measure of CBH and indicates that the boundary layer is well mixed (e.g., Stull and Eloranta 1985). One difference between the results shown in these two figures is how the CBH was determined. The values shown in Fig. 5 are the minimum value of CBH in the averaging period, while the values in Fig. 4c are the average values of CBH.

There is also a relationship between z_{LCL} and the daily average CTH and CTK. The CTH increases with increasing z_{LCL} (Fig. 4c). In other words, clouds with a large CBH tend to also have a large CTH. In contrast, clouds that form during conditions when z_{LCL} is small tend to be thicker than average.

Warren et al. (2007) speculated that the CF would be related to z_{LCL}. Our results suggest that the daily average CF decreases some with increasing z_{LCL} (Fig. 4c). As pointed out in section 4a, changes in the CF can be associated with changes in the CCL, which is also a function of the z_{LCL} (Fig. 4c). The daily average CCL decreases some as the value of z_{LCL} increases above 1.2 km. This suggests that the decrease in CF for cases in

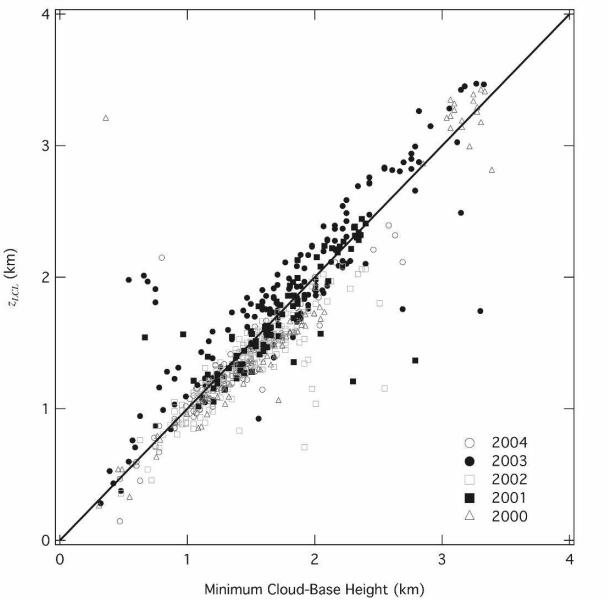

FIG. 5. ARSCL VAP observed minimum cloud-base height vs z_{LCL} computed from the SMOS temperature and dewpoint for 2000 (open squares), 2001 (filled circles), 2002 (asterisks), 2003 (filled squares), and 2004 (triangles). The solid line is the 1:1 line.

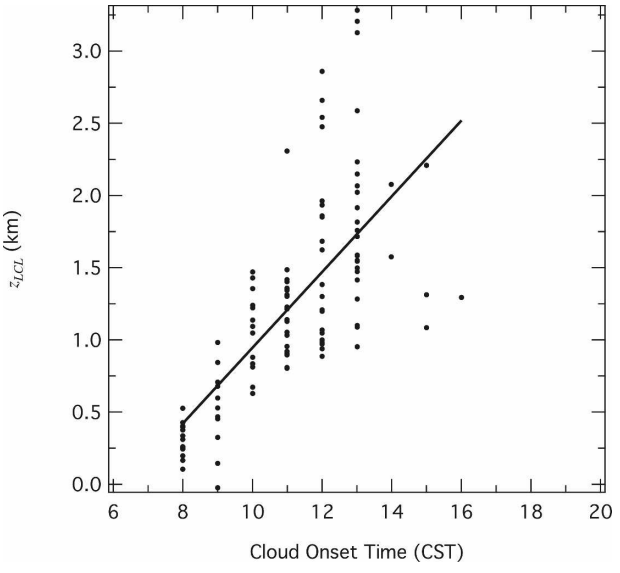

FIG. 6. Cloud onset time as a function of z_{LCL} for the summers 2000 through 2004. The solid line is the least squares best fit to the data.

which the value of z_{LCL} is greater than 1.2 km is due to a decrease in the number of clouds.

Cloud onset time is an important parameter, which describes part of the radiative impacts of FWC. In this study the cloud onset time is defined as the time at which clouds were first observed at the ARCRF SGP Central Facility. It could be argued that these clouds could advect from the region upwind of the Central Facility, but, as shown in Fig. 5, there is good agreement between the observed z_{LCL} at the Central Facility and the CBH. This result indicates that the clouds over the Central Facility are turbulently coupled to the surface and that the cloud onset time is representative of conditions at or near the Central Facility. There is a relationship between z_{LCL} and the cloud onset time (Fig. 6). Wilde et al. (1985) hypothesized that the cloud onset time is a balance between the mixed-layer growth and the z_{LCL}, or range of z_{LCL} values within the boundary layer. Essentially, the first clouds will form whenever the mixed-layer depth grows to the same value as z_{LCL}. In general, when z_{LCL} is small, this should happen more quickly. But, there are a number of additional complications. For example, the rate of growth of the mixed-layer depth is a function of the strength of a nighttime inversion, the surface and entrainment zone fluxes, the static stability of the atmosphere, and the depth of the residual boundary layer, all of which likely leads to much of the scatter in Fig. 6.

d. Day-to-day variation

Analysis of the relationships of the cloud properties to z_{LCL} is difficult to interpret because the value of z_{LCL} changes significantly during the day. To address this problem, the maximum, 75th quartile, median, 25th quartile, and minimum daily values of CBH, CTK, CF, and CCL have been computed and combined into a number of box-and-whisker plots (Fig. 7). Note that the values shown in Fig. 4 and Fig. 7 are not the same because Fig. 4 shows the daily mean values while Fig. 7 shows the daily median values. In this case, median values were used to follow the convention for box-and-whisker plots.

The difference between the maximum and minimum CBH is large, but the range of heights between the 75th and 25th quartiles of CBH over the study period is only about 500 m. There is also variation in the distributions of CBHs from year to year. The two driest years (2001 and 2003) had the highest median CBH and the highest CBH 75th quartile, consistent with the results shown in Fig. 4. However, there is still a significant overlap in CBHs observed during the dry years and the years with more rainfall.

The median CTK is approximately 1 km and the upper and lower quartiles were 0.57 and 1.3 km, respectively. The median CTK values for each year range between 1.3 km and 0.57 km. It is also interesting to note that the summer of 2002 had the largest day-to-day variation in the CTK but had a relatively smaller amount of variation in the CBH. One possible expla-

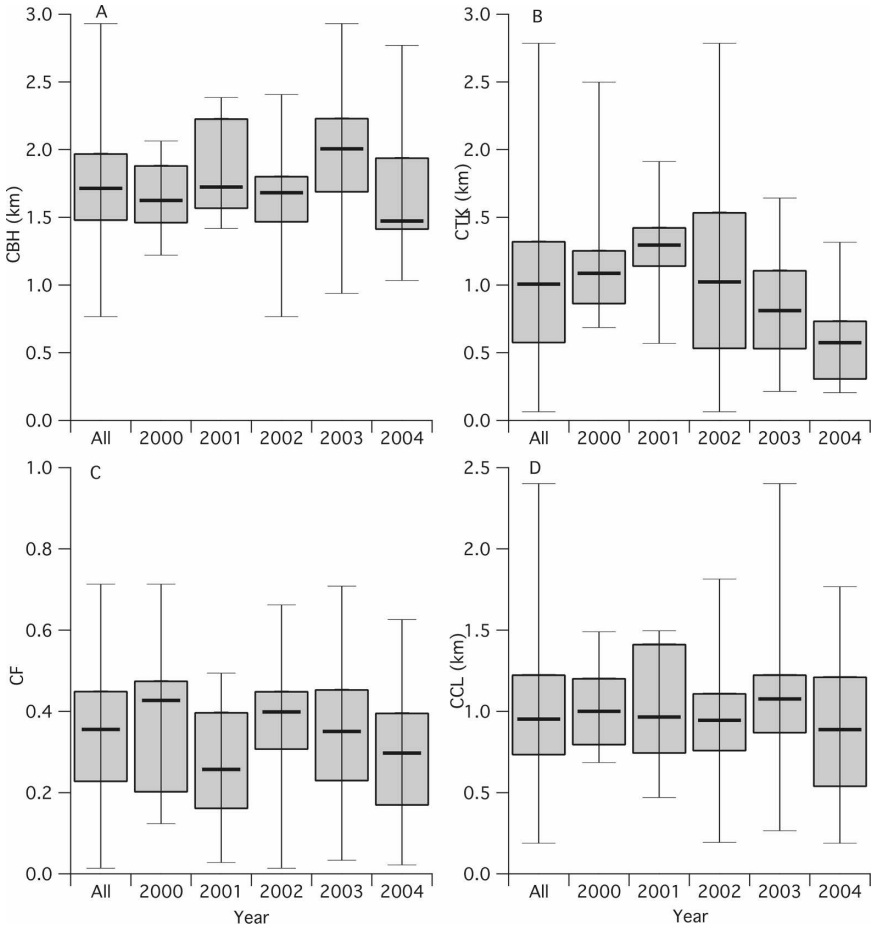

FIG. 7. Box-and-whisker plot of the daily average (a) CHB, (b) CTK, (c) CF, and (d) CCL computed for the entire study period and for each individual summer. The box indicates the 75th and 25th quartile, and the line within the box denotes the median value. The whiskers indicate the maximum and minimum hourly average value.

nation is the relatively large number of hours in 2002 with clouds, which could lead to a larger range of CTH and CTK. As described in section 4b, 2004 had the smallest values of CTK. Indeed, the thickest clouds in 2004 were only as thick as the median found for 2001, and the 25th quartile of CTK measured in 2004 was much smaller than that found for any other year.

The day-to-day variation of the CF over the entire study period is large (Fig. 7c). The range of the 75th and 25th quartile of CF represents a fractional difference of about 64% from the median daily average CF. The variation in daily average CF also changes from year to year. The summer of 2002, which was the wettest summer of the study period, had the smallest range of CF between the 75th and 25th quartiles and one of the larger median values. Attempts to relate the CF to the surface fluxes will be discussed in more detail in section 5.

The daily average CCL generally varies between 1.2 and 0.73 km, or about 28% of the median value of 0.95 km computed for the entire study period. The median value of daily average CCL does not change much from year to year. The summer of 2004 does have more daily average CCL values less than 1 km than the other summers examined in this study. This same summer also had the smallest CTK, and one might expect that shallower clouds are not as wide as deeper clouds.

e. Cloud sensitivity to surface fluxes

A number of other authors (e.g., Betts and Viterbo 2005; Betts 2004; Chagnon et al. 2004; Ray et al. 2003; Rabin et al. 1990) have related the cloud properties to the surface sensible and latent heat fluxes. As described in section 2, the daily average sensible and latent heat flux were computed for the days with FWC. The CBH data and the CF data were then separated into cases with low (less than 250 W m^{-2}) and high (greater than 250 W m^{-2}) of sensible and latent heat fluxes. The data

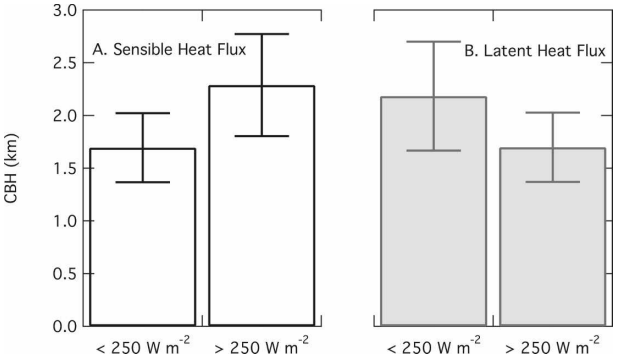

FIG. 8. Daily average CBH as a function of the (a) sensible and (b) latent heat fluxes. Error bars indicate the std dev of the observed fluxes.

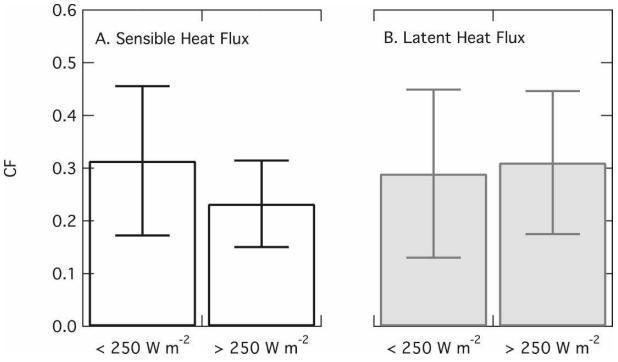

FIG. 9. Same as Fig. 8, but for CF.

was divided in this manner because of the relatively small number of cases with observed FWC and good values of the sensible and latent heat fluxes. A one-sided t test was used in each case to determine if the mean values were different. In these tests the null hypothesis was that means for the large and small flux cases were the same. Figure 8 shows the daily average CBH generally increases with increasing sensible heat flux (p value of 0.001), and decreases with increasing latent heat flux (p value of 0.002). As plotted in Fig. 9, the CF was found to decrease with both increasing and sensible heat flux (p value of 0.008), but does not appear to be strongly related to the latent heat flux (p value of 0.3).

5. Discussion

The formation of FWC is the net result of a number of important atmospheric processes that control both depth and humidity of the boundary layer. In this study, the CF was related to a number of different variables, including the z_{LCL} and surface sensible and latent heat fluxes. One might expect that the cloud fraction would be large when the surface moisture flux is large. However, when the moisture flux is large, the sensible heat flux is generally small (not shown), and the boundary layer depth is likely suppressed and the boundary layer depth may not grow as high as z_{LCL}. In contrast, clouds can form even when the moisture flux is very small because the boundary layer may grow to great depth. Additional factors, including subsidence caused by large-scale circulations, affect the formation of shallow clouds.

a. Cloud fraction and days with cloud cover

Chagnon et al. (2004) found that the CF increases with increasing sensible heat flux. At first glance, this appears to contradict the findings presented here (Fig. 9), but this difference can be explained with a closer look at the methods used to compute the average CF. In this study, the CF is the arithmetic average of observed CF for days during which there were clouds (section 2), it does not account for the number of days with or without FWC. In contrast, the study of Chagnon et al. (2004) used CF compounded over a long time interval. This measure is similar to the concept of cloud-cover hours suggested by Stull (1992), which he defined to be the CF multiplied by the amount of time with that CF, and the concept of the average cloud amount described by Warren and Hahn (2002), which they defined as the product of the frequency-of-occurrence and the amount-when-present. A similar methodology has been applied to the data from the Central Facility. While the year-to-year variability of the CF is generally small, the year-to-year variability of cloud-cover hours is quite large (Table 1). But, it does not appear that this variability is related to the amount of precipitation falling near the Central Facility. Both 2001 and 2003 had less than normal precipitation at the Central Facility, but 2001 had the smallest value of cloud-cover hours,

TABLE 1. Number of hours with clouds, cloud-cover hours, and mean cloud fraction for all cases: cases separated by years and cases separated by z_{LCL} category.

Category	Hours with clouds	Cloud-cover hours	CF
All	611	195.96	0.32
2000	78	27.07	0.33
2001	75	18.24	0.24
2002	217	68.04	0.32
2003	153	52.86	0.35
2004	88	29.74	0.34
$z_{\mathrm{LCL}} < 1.2$ km	153	60.58	0.39
1.2 km $< z_{\mathrm{LCL}} <$ 1.6 km	246	73.94	0.30
1.6 km $< z_{\mathrm{LCL}}$	197	56.09	0.29

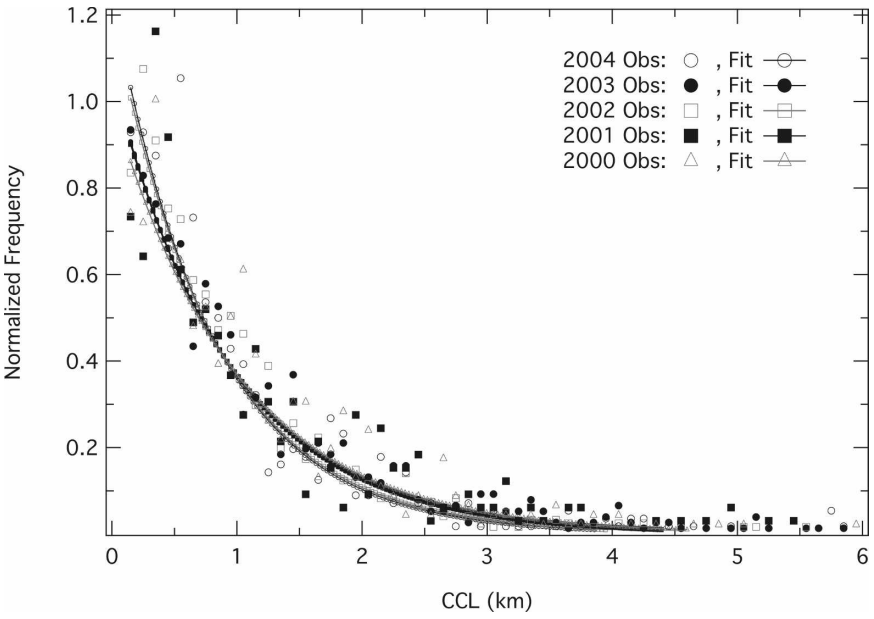

FIG. 10. Distributions of CCL for the summers 2000 (triangles), 2001 (filled squares), 2002 (open squares), 2003 (filled circles), and 2004 (open circles). Lines and small symbols correspond to the best-fit exponential distribution for each year.

while 2003 had the second largest amount of cloud-cover hours.

While the CF shows a decreasing trend with increasing z_{LCL}, the total number of hours with FWC and the cloud-cover hours do not. Both total number of hours and the cloud cover are greatest for cases in which z_{LCL} is between 1.2 and 1.6 km (Table 1). The cloud-cover hours are about the same for cases in which z_{LCL} was less than 1.2 km or was greater than 1.6 km, although there were many more hours in which z_{LCL} was greater than 1.6 km than there were hours in which z_{LCL} was less than 1.2 km. These results imply that, when z_{LCL} is less than 1.2 km, clouds are less likely to form but, if they do form, then many clouds form, leading to a relatively large CF. In contrast, when z_{LCL} is greater than 1.6 km, clouds are more likely to form, but only a few clouds form so that the CF is smaller. Therefore, our results are consistent with the findings of Chagnon et al. (2004).

b. Distributions of CCL

A number of authors have examined distributions of CCL (e.g., Plank 1969; Cahalan and Joseph 1989). These efforts have focused on different case studies, rather than multiyear averages. To help address these shortcomings, histograms of CCL were calculated for each year (Fig. 10) and for the three different categories of z_{LCL} (Fig. 11). There has also been some discussion in the literature in regards to the shape of the histogram of CCL. For example, Plank (1969), Hozumi et al. (1982), and Lane et al. (2002) fit exponential distributions to their observed histograms. Other authors have suggested either a single power law (Machado and Rossow 1993) or a double power law (Cahalan and Joseph 1989; Benner and Curry 1998; Sengupta et al. 1990). We use an exponential distribution to fit our observations. This distribution is defined as $F = A\exp(-Al)$, where F is the normalized frequency, l is the CCL, and A is the best-fit parameter, has been fit to the data. The value of A determines how quickly the distribution decreases with CCL, and the mean of the distribution is A^{-1}. In our study, the mean CCL ranges form approximately 1.0 to 1.2 km (Table 2). We also fit a double power law to the CCL distributions, but the value of the χ^2 statistic is smaller for the exponential fits, so only results for the exponential fit are shown. Each of the yearly distributions was compared to each other using the Kolmogorov–Smirnov test (Press et al. 1992). This test indicates that the distributions from 2002 and 2004 are significantly different from the distributions constructed from data collected during 2000, 2001, and 2003 at the 0.05 level. Likewise the distributions for the various z_{LCL} groups were also compared. While the differences in the distributions are subtle, the Kolmogorov–Smirnov test indicates that the differences are statistically significant. It is not immediately clear why the CCL distributions fall into these two distinct groups, especially since 2001 and 2003 are the dry years at the Central Facility.

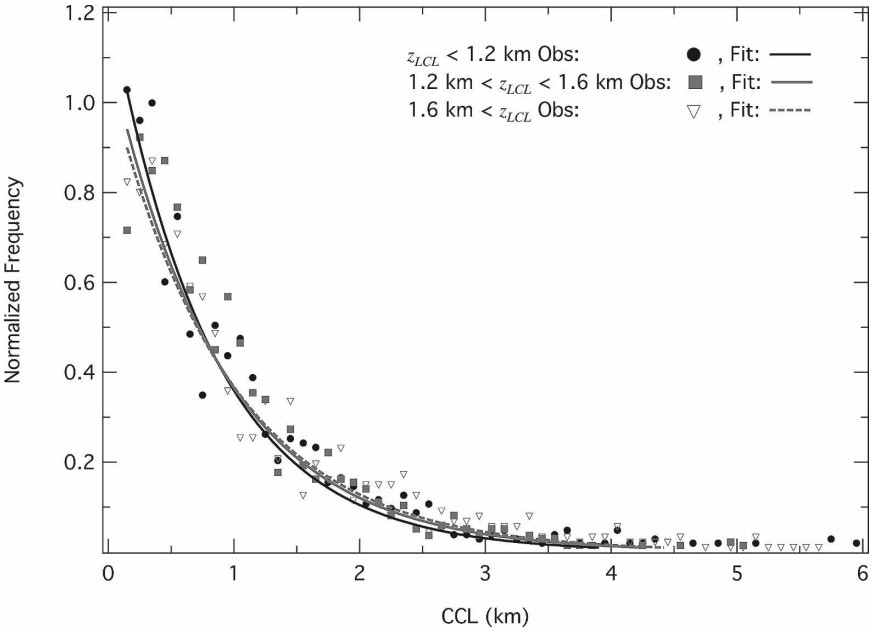

FIG. 11. Normalized histogram of CCL for each z_{LCL} group (symbols) and the least squares best-fit exponential distribution (lines).

c. Relationship between CCL and CF

A number of authors have examined the contribution to the CF from clouds of various sizes. In a study of shallow clouds over Florida, Rodts et al. (2003) found that the smallest clouds contributed the most to the cloud fraction. This is in contrast to a number of other observational and modeling studies that found there to be a small range of cloud sizes that contributed the most to the CF (e.g., Plank 1969; Wielicki and Welch 1986; Sengupta et al. 1990; Neggers et al. 2003). Rodts et al. attributed these differences to the one-dimensional sampling they used in their analysis compared to the two-dimensional sampling that was used in other studies. We computed distributions of α_f (section 2) using all of the CCL data collected at the Central Facility for the five summers of interest. Similar to the data collected by Rodts et al. (2003), data presented here is one-dimensional except that the information about the vertical distribution of CF is lacking, similar to data collected with other remote sensors. In contrast to the results presented by Rodts et al. (2003), but similar to the results found in other studies (e.g., Plank 1969; Wielicki and Welch 1986; Sengupta et al. 1990; Neggers et al. 2003), we found that CCL that contributed the most to the CF was for an intermediate cloud size of about 1 km (Fig. 12). This size is often referred to as the dominant cloud size. The smallest clouds were found to contribute very little to the CF. In addition, the data has been sorted by time, 1000–1200, 1200–1400, and 1400–1600 CST, to determine if the contribution to the CF changes with the time of day (Fig. 12). These results indicate the dominate CCL does not change much throughout the day, in agreement with the relatively small change in the mean CCL (Fig. 4a).

TABLE 2. Exponential fit parameters for each summer and for each z_{LCL} category.

Category	Best-fit A (km^{-1})	Std dev
2000	1.0	0.054
2001	1.1	0.070
2002	1.2	0.047
2003	1.1	0.034
2004	1.2	0.067
$z_{\mathrm{LCL}} < 1.2$ km	1.2	0.047
1.2 km $< z_{\mathrm{LCL}} <$ 1.6 km	1.1	0.053
1.6 km $< z_{\mathrm{LCL}}$	1.1	0.037

In their detailed analysis, Rodts et al. (2003) suggested a number of reasons for the difference between the one-dimensional (aircraft) and two-dimensional (remote sensors) distributions of the cloud fraction density. Some differences are induced because a one-dimensional aircraft sampling technique rarely passes through a cloud center and is more likely to detect large clouds. They were able to account for these differences analytically. An additional factor that they discussed is the influence of complicated cloud geometries on cloud properties determined in situ, such as from a research aircraft, and those determined using a remote sensing

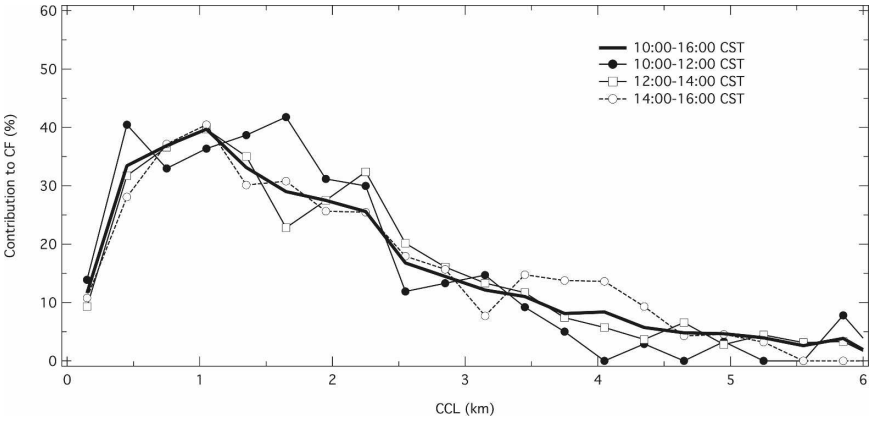

FIG. 12. Normalized density of CF, defined as $\alpha_f(l)$/CF, by various CCL for periods between 1000 and 1600 CST (thick solid line), 1000 and 1200 CST (solid circles), 1200 and 1400 CST (open squares), and 1400 and 1600 CST (open circles) (similar to Rodts et al. 2003; Fig. 8).

instrument, such as a satellite. Real clouds can have complicated shapes, tilt, or overlap making interpretation difficult. An aircraft flying through a cloud field might identify separate towers from the same cloud as two different smaller clouds. Remote sensing instruments combine clouds that tilt, overlap, or lie very close together into larger clouds. The time resolution of the ARSCL VAP is 10 s, so small gaps between clouds might be missed, which would lead to an overestimate of the number of long CCL. For example, if we assume that the wind speed at cloud base is 7 m s^{-1} (approximately the average wind speed at cloud base for the five summers), then gaps smaller than 70 m might be missed by the ARSCL VAP. In addition, our data likely underestimates the number of short CCL. The problem arises when the cloud exists in only one ARSCL VAP observation, and it is impossible to determine the CCL. However, we see that the decrease in α_f occurs for a number of bins below the peak, not just the bin with the smallest CCL, so it is unlikely that adding more CCLs to the bin with the smallest CCL would alter our results. In many ways our dataset is very similar to the satellite observations because we sense the projection of a cloud remotely, and it is interesting to note that the distributions observed were similar to those gathered using other remote sensing techniques. Our results suggest that the differences in the dominant cloud size induced by the complicated cloud geometry are more important than the dimension of the measurement.

6. Conclusions

A detailed 5-yr climatology of FWC above the Central Facility has been presented. Cloud properties were determined using the ARSCL VAP, which combines data from the 35-GHz cloud radar, micropulse lidar, and laser ceilometer to estimate the cloud-base height (CBH), cloud-top height (CTH), cloud thickness (CTK), and cloud fraction (CF). Data from the 915-MHz wind profiler was combined with the ARSCL VAP in order to estimate the cloud-chord length (CCL). There was a significant diurnal evolution to the CBH, which tended to increase throughout the day, and the CTK, which tended to decrease with time. The latter was largely due to the increase in CBH because the CTH did not change much throughout the day. The CF increased through the morning and into the afternoon, reaching its peak value near 1400 CST. The CCL was nearly constant throughout the day. Since CF is a function of CCL and the number of clouds, the results that we obtained (that the CF is variable and the CCL is nearly constant) suggests that the number of clouds has a diurnal evolution similar to the CF.

The effect of the year-to-year variations of precipitation and day-to-day variation of the surface sensible and latent heat fluxes and z_{LCL} on the cloud macroscale properties was also investigated. While there were differences in some cloud properties from year to year, with the exception of the CBH, these differences did not seem to be related to the amount of precipitation. The daily mean values of CBH, CF, and CCL varied significantly and were found to be sensitive to z_{LCL}. When z_{LCL} is relatively small the CBH tends to be smaller than average, and the opposite is true for large values of z_{LCL}. Larger values of CCL are associated with small values of z_{LCL}. While the CF was larger for small values of z_{LCL}, the total cloud-cover hours were greatest for moderate values of z_{LCL}. Our findings suggest that, when z_{LCL} is small, clouds are less likely to form than when z_{LCL} is large, but if FWC do form when

z_{LCL} is small many clouds form, leading to a relatively large CF. The CBH and CF were found to be sensitive to the surface sensible and latent heat fluxes When the sensible heat flux is large the CBH tend to be larger and the CF tends to be smaller than for cases in which the flux is small. When the latent heat flux is large, the CBH tended to be smaller, but the CF was found to not change significantly.

Distributions of CCL were also examined. Similar to previous results (e.g., Plank 1969; Wielicki and Welch 1986; Sengupta et al. 1990; Neggers et al. 2003), we found that the distributions of CCL described by an exponential fit are robust. There were some statistically significant differences from year to year, but they did not seem to be related to the amount of precipitation. The contribution of clouds with various CCL to the CF was also determined, with clouds having a CCL near 1 km contributing the most to the CF. This value, based on surface observations, is larger than the dominant cloud size determined using aircraft-based measurements of Rodts et al. (2003), but is similar to other studies that have made use of other remote sensing techniques (e.g., Plank 1969; Wielicki and Welch 1986; Sengupta et al. 1990).

This 5-yr climatology of FWC can provide a constraint on new cumulus parameterizations that account for shallow clouds. Also, the application of this climatology and related approaches can improve our understanding of the effects that FWC have on the surface radiative budget and heating profiles.

Acknowledgments. This research was supported by the Office of Biological and Environmental Research of the U.S. Department of Energy (DE-AC05-76RL01830) as part of the Atmospheric Radiation Measurement Program and as part of the Atmospheric Measurement Program Climate Research Facility. Pacific Northwest National Laboratory is operated for the U.S. Department of Energy by Battelle Memorial Institute. Comments from two anonymous reviewers greatly improved the manuscript.

APPENDIX

List of Acronyms

ABRFC	Arkansas–Red River Basin Forecast Center
ACRF	ARM Climate Research Facility
ARM	Atmospheric Radiation Measurement Program
ARSCL	Active Remotely Sensed Clouds Locations
CAPE	Convective available potential energy
CBH	Cloud-base height
CCL	Cloud-chord length
CF	Cloud fraction
CINE	Convective inhibition energy
CTH	Cloud-top height
CTK	Cloud thickness
EBBR	Energy Balance Bowen Ratio
ECMWF	European Centre for Medium-Range Weather Forecasts
FWC	Fair-weather clouds
SGP	Southern Great Plains
SMOS	Surface Meteorological Station
VAP	Value-added product

REFERENCES

Benner, T. C., and J. A. Curry, 1998: Characteristics of small tropical cumulus clouds and their impact on the environment. *J. Geophys. Res.,* **103,** 28 753–28 767.

Berg, L. K., and R. B. Stull, 2002: Accuracy of point and line measures of boundary layer cloud amount. *J. Appl. Meteor.,* **41,** 640–650.

——, and ——, 2005: A simple parameterization coupling the convective daytime boundary layer and fair-weather cumuli. *J. Atmos. Sci.,* **62,** 1976–1988.

Betts, A. K., 2004: Understanding hydrometeorology using global models. *Bull. Amer. Meteor. Soc.,* **85,** 1673–1688.

——, and P. Viterbo, 2005: Land-surface, boundary-layer, and cloud-field coupling over the southwest Amazon in ERA-40. *J. Geophys. Res.,* **110,** D14108, doi:10.1029/2004JD005702.

Bohren, C. F., and B. A. Albrecht, 1998: *Atmospheric Thermodynamics.* Oxford University Press, 402 pp.

Cahalan, R. F., and J. H. Joseph, 1989: Fractal statistics of cloud fields. *Mon. Wea. Rev.,* **117,** 261–272.

Chagnon, F. J. F., R. L. Bras, and J. Wang, 2004: Climatic shift in patterns of shallow clouds over the Amazon. *Geophys. Res. Lett.,* **31,** L24212, doi:10.1029/2004GL021188.

Clothiaux, E. E., T. P. Ackerman, G. Mace, K. P. Moran, R. T. Marchand, M. Miller, and B. E. Martner, 2000: Objective determination of cloud heights and radar reflectivites using a combination of active remote sensors at the ARM CART sites. *J. Appl. Meteor.,* **39,** 645–665.

Dong, X., P. Minnis, and B. Xi, 2005: A climatology of midlatitude continental clouds from the ARM SGP Central Facility. Part I: Low-level cloud macrophysical, microphysical, and radiative properties. *J. Climate,* **18,** 1391–1410.

Duchon, C. E., and M. S. O'Malley, 1999: Estimating cloud type from pyranometer observations. *J. Appl. Meteor.,* **38,** 132–141.

Hozumi, K., T. Harimaya, and C. Magono, 1982: The size distribution of cumulus clouds as a function of cloud amount. *J. Meteor. Soc. Japan,* **60,** 691–699.

Kassianov, E., C. Long, and M. Ovtchinnikov, 2005: Cloud sky cover verses cloud fraction: Whole-sky simulations and observations. *J. Appl. Meteor.,* **44,** 86–98.

Lane, D. E., K. Goris, and R. C. J. Somerville, 2002: Radiative transfer through broken clouds: Observations and model validation. *J. Climate,* **15,** 2921–2933.

Lazarus, S. M., S. K. Krueger, and G. G. Mace, 2000: A cloud climatology of the Southern Great Plains ARM CART. *J. Climate,* **13,** 1762–1775.

Machado, L. A. T., and W. B. Rossow, 1993: Structural charac-

teristics of radiative properties and tropical cloud clusters. *Mon. Wea. Rev.,* **121,** 3234–3260.

Neggers, R. A. J., H. J. J. Jonker, and A. P. Siebesma, 2003: Size statistics of cumulus cloud populations in large-eddy simulation. *J. Atmos. Sci.,* **60,** 1060–1074.

Peppler, R. A., and P. J. Lamb, 1989: Tropospheric static stability and central North American growing season rainfall. *Mon. Wea. Rev.,* **117,** 1156–1180.

Plank, V. G., 1969: The size distribution of cumulus clouds in representative Florida populations. *J. Appl. Meteor.,* **8,** 46–67.

Press, W. H., S. A. Teukolsky, W. T. Vetterling, and B. P. Flannery, 1992: *Numerical Recipes in C: The Art of Scientific Computing.* 2nd ed. Cambridge University Press, 994 pp.

Rabin, R. M., S. Stadler, P. J. Wetzel, D. J. Stensrud, and M. Gregory, 1990: Observed effects of landscape variability on convective clouds. *Bull. Amer. Meteor. Soc.,* **71,** 272–280.

Randall, D., M. Khairoutdinov, A. Arakawa, and W. Grabowski, 2003: Breaking the cloud parameterization deadlock. *Bull. Amer. Meteor. Soc.,* **84,** 1547–1564.

Ray, D. K., U. S. Nair, R. W. Welch, Q. Han, J. Zeng, W. Su, T. Kikuchi, and T. J. Lyons, 2003: Effects of land use in Southwest Australia: 1. Observations of cumulus cloudiness and energy fluxes. *J. Geophys. Res.,* **108,** 4414, doi:10.1029/2002JD002654.

Rodts, S. M. A., P. G. Duynkerke, and H. J. J. Jonker, 2003: Size distributions and dynamical properties of shallow cumulus clouds from aircraft observations and satellite data. *J. Atmos. Sci.,* **60,** 1895–1912.

Sengupta, S. K., M. S. Navar, D. W. Chen, R. M. Welch, and T. A. Berendes, 1990: Cumulus cloud field morphology and spatial patterns derived from high spatial resolution Landsat imagery. *J. Appl. Meteor.,* **29,** 1245–1267.

Stokes, G. M., and S. E. Schwartz, 1994: The atmospheric radiation measurement (ARM) program: Programmatic background and design of the Cloud and Radiation Test Bed. *Bull. Amer. Meteor. Soc.,* **75,** 1201–1221.

Stull R. B., 1988: *Introduction to Boundary Layer Meteorology.* Kluwer Academic, 666 pp.

——, 1992: Impact of boundary-layer clouds—A case study of cover hours. *J. Climate,* **5,** 390–394.

——, and E. Eloranta, 1985: A case study of the accuracy of routine, fair-weather cloud-base reports. *Natl. Wea. Dig.,* **10,** 19–24.

——, E. Santoso, L. Berg, and J. Hacker, 1997: Boundary Layer Experiment 1996 (BLX96). *Bull. Amer. Meteor. Soc.,* **78,** 1149–1158.

Wang, D., M. B. Smith, Z. Zhang, S. Reed, and V. I. Koren, 2000: Statistical comparison of the mean areal precipitation estimates from WSR-88D, operational and historical gage networks. Preprints, *15th Conf. on Hydrology,* Long Beach, CA, Amer. Meteor. Soc., 2.17.

Wang, Z., and K. Sassen, 2001: Cloud type and macrophysical property retrieval using multiple remote sensors. *J. Appl. Meteor.,* **40,** 1665–1682.

Warren, S. G., and C. J. Hahn, 2002: Cloud climatology. *Encyclopedia of Atmospheric Sciences,* J. R. Holton, J. Pyle, and J. A. Curry, Eds., Academic Press, 476–483.

——, ——, J. London, R. M. Chervin, and R. L. Jenne, 1988: Global distribution of total cloud cover and cloud type amounts over the ocean. NCAR Tech. Note, NCAR/TN-317+STR, 41 pp.

——, R. M. Eastman, and C. J. Hahn, 2007: A survey of changes in cloud cover and cloud types over land from surface observations, 1971–96. *J. Climate,* **20,** 717–738.

Wielicki, B. A., and R. M. Welch, 1986: Cumulus cloud properties derived using Landsat satellite data. *J. Climate Appl. Meteor.,* **25,** 261–276.

Wilde, N. P., R. B. Stull, and E. W. Eloranta, 1985: The LCL zone and cumulus onset. *J. Climate Appl. Meteor.,* **24,** 640–657.

Young, C. B., A. A. Bradley, W. F. Krajewski, A. Kruger, and M. L. Morrissey, 2000: Evaluating NEXRAD multisensor precipitation estimates for operational hydrologic forecasting. *J. Hydrometeor.,* **1,** 241–254.